INITIAL DETECTION OF LOW EARTH ORBIT OBJECTS THROUGH PASSIVE OPTICAL WIDE ANGLE IMAGING SYSTEMS

T. Hasenohr [*, 1, 2], D. Hampf[1], P. Wagner[1], F. Sproll[1], J. Rodmann[1], L. Humbert[1], A. Herkommer[2], W. Riede[1],

[1]German Aerospace Center (DLR), Institute of Technical Physics, Pfaffenwaldring 38-40, 70569 Stuttgart, Germany

[2]University of Stuttgart, Institute of Applied Optics, Pfaffenwaldring 9, 70569 Stuttgart, Germany

Abstract

For surveillance of the low Earth orbit (LEO) population the orbits of resident space objects (active satellites or space debris) has to be known and cataloged. A possible solution for initial detection is the passive optical observation through wide-angle imaging systems with large fields of view (FOV). Based on measurements of these systems a short-time prediction of the object's trajectory can be determined which is sufficiently accurate to recapture it with a high resolution telescope during the pass of the object.

This paper presents the "Stare and Chase" wide-angle system for initial LEO object detection and determination developed by the German Aerospace Center (DLR) at the Satellite-Laser-Ranging station at the Uhlandshöhe in Stuttgart. The performance of the "staring" camera is shown based on the simulation tool PROOF by ESA and compared with real measurements. Finally the recapture of space debris without prior information is presented.

1. INTRODUCTION

The growing number of space debris objects in low Earth orbit causes an increasing risk for active satellites and manned space missions. A collision in space does not only affect the operational work of a satellite. It can also cause a sudden expansion of the debris population, which increases the threat for spacecraft even more. In 2007 the Chinese anti-satellite test and the accidental collision of the active Iridium 33 and the defunct Cosmos 2251 in 2009 have enhanced the number of debris in LEO by about 60 % [1]. These two events are responsible for four of six close approaches of debris to the International Space Station in just 12 months (April 2011 to April 2012) where four collision avoidance maneuvers were necessary [2].

In order to avoid accidental collisions precise orbital information on resident space objects (RSO) is required. Therefore the U.S. Space Surveillance Network (SSN) maintains a catalog containing over 40000 RSOs where more than 17200 are still in orbit [3]. Due to the sensitivity of the detectors the minimum cataloged size for cataloged debris is limited to about 10 cm for LEO objects and 70 cm for pieces in the geostationary Earth orbit (GEO) [4]. About 85 % of the 17200 entries in this database are available as Two Line Element (TLE) catalog by the North American Aerospace Defense Command (NORAD) [11]. This makes it necessary to complement this catalog by initial detection of the missing RSOs for third parties.

* Corresponding author:
Email address: thomas.hasenohr@dlr.de

Radars are the most common systems for LEO surveillance i.a. due to the independence of weather conditions. However, passive optical systems can be very efficient for LEO observations as well [5] despite the fact that these have been developed mostly for GEO surveillance. Passive optical systems are using the sun as illumination source and are able to detect small objects in LEOs as long as they are not in Earth's shadow. Unlike radar systems, space debris telescopes are cost effective and can operate unmanned like the French TAROT telescopes [6].

A system for initial detection of RSOs must be able to cover large regions of the sky for detecting as many crossing objects as possible. The initial detection and subsequent precise measurements of the object's trajectory, which requires high image resolutions, have to take place during the same overpass. Otherwise, not sufficient information is known for adding the object to a catalog. Using wide FOV telescopes [7, 8] with FOVs of up to about 10° are one method for precise position measurements of unknown RSOs. In order to reach large observed regions it is also possible to use multiple apertures with smaller FOVs [9]. A third possibility is used by the DLR in Stuttgart. Here an astronomical camera equipped with a telephoto lens is used for initial detection (staring). Afterwards a high resolution telescope is guided to the new detected RSO (chasing) to perform accurate measurements. Such a system can be set up with commercial of the shelf (COTS) components and is able to reach FOVs up to 15.5°× 15.5°.

In the following this paper presents the operation of the "Stare and Chase" system, its hardware and software. Performance simulations of the "staring" system are shown and compared to real measurements. Finally, the successful recapturing of objects without prior information

is reported and an outlook is given for upgrading the system.

2. THE STARE AND CHASE SYSTEM

2.1. Stare and Chase

The "Stare and Chase" system is a passive optical approach for initial detection and tracking of objects in LEO. Main components are an astronomical camera with a telephoto lens which serves as wide angle imaging sensor, a 17 inch (432 mm) telescope on an astronomical mount for precise angular coordinate measurements and a computer system for image processing and telescope control (Figure 1).

Figure 1: Stare and Chase assembly: The staring camera is used for initial detection of RSOs, while the telescope recaptures the detected objects for precise measurements.

An astronomical camera equipped with an exchangeable, COTS lens "stares" into the night sky in a specific direction and takes images continuously with typical exposure times in the range of 0.05 s to 1 s. The short focal length of the staring system leads to a wide FOV and therefore a large observed region of the sky compared to telescopes. During the crossing of the FOV by an object, an image processing algorithm extracts the object's position and determines if it is already contained in the TLE catalog. Furthermore a short time prediction of the estimated object's trajectory is calculated giving the equatorial coordinates after a specific time. For recapture the object, the predicted coordinates are forwarded to the high resolution telescope. The camera of the high resolution telescope takes an image exactly at the time corresponding to the prediction. This enables a high resolution measurement of the angular coordinates of the initially unknown object. Subsequent laser ranging e.g. with a system presented in [10] could allow generating even more precise orbit information.

The presented method can be used to set up a database or maintaining an existing one. For catalog maintenance the algorithm can be adjusted to track only unknown objects by the telescope or objects for which the available information is invalid.

For a passive optical staring system detecting space debris the most important parameters are the following:

- FOV: Gives the size of the observed region in the sky. The larger the area the more detections are possible.
- Pixel scale: The higher the resolution of the image the more accurate the short-time prediction for the recapturing can be.

- Aperture: A larger aperture allows detections of fainter objects.
- Frame rate: If the frame rate increases for a specific time span, the information about the location of an object increases which leads to a higher precision of the prediction. However, the image processing time limits the useful frame rate.
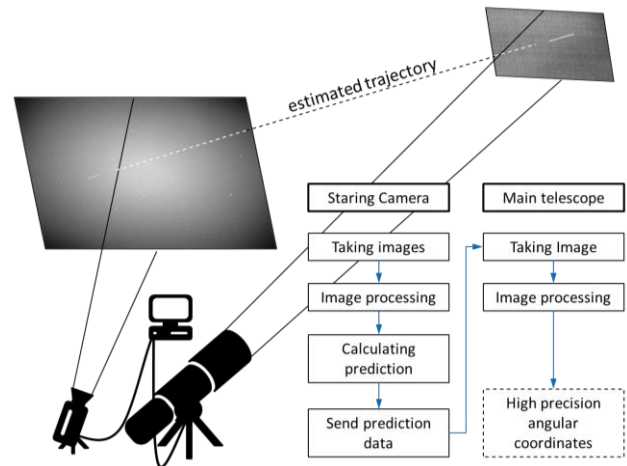

Figure 2: Sequence diagram of the Stare and Chase system (right) and the simplified telescope system design (left).

In contrast to wide field telescopes for initial detection of RSOs the presented system is set up with COTS components. Thus this cost effective solution can be easily assembled by a third party.

A combination of low costs and the possibility to implement the staring system at already operating telescopes allows setting up a global network of optical space surveillance systems at different locations. This guarantees an observation possibility of LEOs. Furthermore it would eliminate the disadvantages of the dependence on weather conditions and limited observation times.

2.2. Hardware

Two different staring cameras were investigated. The first is the ProLine 16803 from Finger Lakes Instrumentation (FLI). Its sensor is a CCD which is optimized for low noise. The second camera is a Zyla from Andor. It is a CMOS senor chip with the advantage of a fast readout. Specific data of the two cameras are shown in Table 1. Both cameras are installed on an azimuth-elevation mount which is aligned to a fixed direction.

Table 1: Parameters of the Staring Cameras

Parameter	FLI PL16803	Andor Zyla
Sensor	CCD (Front Illuminated)	CMOS (Front Illuminated)
Pixels	4096 × 4096	2560 × 2160
Pixel Size	9 µm	6.5 µm
Sensor Size	36.8 mm × 36.8 mm	16.6 mm × 14.0 mm
Readout Noise	14 e$^-$/ px	2.9 e$^-$/ px
Dark Current	0.005 e$^-$/ px/ s	0.14 e$^-$/ px/ s
Maximum Quantum Efficiency	60 %	60 %
Interface	USB2.0	Camera Link
Gap time (simulation)	4 s	2 s

A large pixel size of the FLI camera allows detecting faint objects. This pixel size and the high number of pixels together with the used lenses are leading to a wide FOV. A disadvantage of this camera is the mechanical shutter which needs almost 40 ms for opening and closing. This delay can cause inaccuracies in the predicted location for recapturing. The pixel size of the Andor Zyla camera is smaller which results in less collected light reflected by an RSO per pixel. For short exposure times the low readout noise compensates this disadvantage. An overall smaller sensor leads to a smaller FOV compared to the FLI camera. However, a fast readout speed allows high frame rates which can be useful for multiple detections of fast objects. Furthermore it has an electronic shutter which does not cause a delay of the exposures.

Several types of camera lenses can be attached to the staring cameras. This allows adjusting the staring system to potential applications. For detecting faint objects large apertures are advantageous which usually correspond to longer focal lengths. A camera lens with a short focal length can be used if a wide FOV is necessary. Tests were performed with different lenses for developing the system. Optical parameters of these lenses are 50mm (focal length) f/1.2 (focal length/ aperture diameter), 85mm f/1.2, 135mm f/1.2, 135mm f/2 and 200mm f/2. A combination of these lenses and the presented cameras give FOVs in the range from 4.0° × 4.75° to 36.40° × 36.40°.

Table 2: Lenses with parameters used in the simulations.

No. of lens	Focal length	Aperture diameter	F-number
1	50	41.7	1.2
2	85	70.8	1.2
3	135	112.5	1.2
4	135	67.5	2.0
5	200	100.0	2.0

The high resolution telescope from PlaneWave is a corrected Dall-Kirkham type with an aperture diameter of 17 inch (432 mm) and focal length of 2939 mm mounted on an equatorial telescope mount. A FOV of 0.32° × 0.27° and a resolution of 0.5 arcseconds per pixel are reached with the sCMOS camera Andor Zyla (same model as for staring system) as imaging sensor.

Necessary for location predictions of detected RSOs are precise time stamps in the range of 5 ms to 10 ms. In order to guarantee this timing accuracy the trigger of the staring cameras and the telescope camera are synchronized to the GPS time.

2.3. Software

The used software has to be able to detect RSOs on a star background, give an accurate prediction of a future location and control the astronomical telescope, which is discussed in more detail in the following sections.

2.3.1. Object determination

Depending on the exposure times of the staring camera there are two different methods of object detection used. For longer exposures (>0.5 s) an object crossing the FOV causes a track in the image. This makes it possible to separate between objects and stars (imaged as dots)

based on the shape. Exposure times shorter than about 0.5 s need another analysis. Here the RSOs causing dots as well and have to be identified by their movement. The advantage of using shorter exposure times is the better signal-to-noise ratio in the images.

For a later transformation from pixel coordinates of the image into the right ascension-declination system a star map is generated which contains the astrometry for each image. This is realized by the astrometric engine PinPoint. Therefore the exact astronomic coordinates of each pixel are known.

Two successive images for detecting a track are used by the algorithm which can handle longer exposure times. The first image is subtracted from the second image to eliminate vignetting effects caused by the camera lens. This approach is used because it is faster than a vignetting filter algorithm. Flat fielding would also be a fast solution for this problem and can be implemented in future versions. Following this, the image is binarized with an adjustable threshold (for the measurements later a standard deviation of 2 was used) above the background noise. Now all remaining structures can be analyzed in respect of their shape. A structure is declared as an object if the aspect ratio is greater than a specific factor (depending on the exposure time and the used lens). The orientation and location of the track give information if the same object was detected in an earlier image. Two successive detections of the same object lead to the direction of the trajectory and a prediction about a future location can take place.

For short exposure times a different approach is used. The shape of an object does not differ from the shape of a star. Hence, three images are necessary to determine an object reliably. Each image is analyzed for structures the same way as for long exposure times. This time each structure is assigned to its right ascension- and declination coordinate and compared to the coordinates occurring in the image before. The coordinates do not change and will be deleted if the structure is a star. In the end just moving objects remain. A third image is used to decrease the risk of fault detections caused by stars occurring not in every image. This appears e.g. due to faint stars close to the threshold level of the binarization. The known coordinate information of each structure in the first two images allows generating a region where a possible object should be in the third image. Three different equatorial coordinates of the structure in the three images and a location in one of the regions in the third image declares the structure to an orbiting object.

2.3.2. Trajectory estimation

For both, long and short exposure times of the staring camera, the prediction of the RSOs future location is similar. The only difference is the number of available coordinates. For long exposure times starting and end points of two tracks are known which gives four locations and the time between those. Short exposures, where three images are used for detection, are giving the information about the location of the center of gravity of each object dot. In total three locations with three timestamps are available. In both cases are the locations extracted in pixel coordinates of the image and a straight line is fitted to them. The interception point where the

telescope recaptures the RSO is calculated through the time gap and distance between the very first and last location coordinate and the chosen time until interception (in the following: headtime). A typical headtime is in the range of 10 s and 15 s. Based on the coordinate plate generated during the image processing the predicted location in pixel coordinates can be translated into the right ascension-declination system. This information together with the time of interception is sent to the telescope control.

The functionality of this detection algorithm and recapturing of RSOs is presented in Chapter 4.2.

3. SIMULATIONS

In order to evaluate the performance of the staring system, analyzes were done with the simulation software PROOF by ESA. This tool simulates an observation campaign of an optical or radar based observation facility. It uses the ESA's space debris environment MASTER [12] (latest update 2009) as space population model. PROOF simulates crossings of RSOs through the FOV of the system and determines detected objects in respect to the system parameters.

Adjustable system parameters for the following simulations are shown in Table 3. Some depend on the used camera, lens or the different combinations of them respectively. These are given for each simulation separately or are contained in Table 1 or Table 2. Quantum efficiency of the camera sensor and the atmospheric absorption can be adjusted as well. However, weather conditions and atmospheric turbulences are neglected. The latter one can be considered in adjusting the point spread function (PSF) parameter of the camera lens.

The detection efficiency is the ratio of detected objects to all objects crossing the FOV and is a function of the size. Prior simulation showed that during April (September as well) the longest optical observation campaigns to LEO objects can be conducted for a system pointing to zenith [13]. Shorter observation times occur in the summer months, while gaps in RSOs illumination appear in the winter months as a result of Earth's shadow. For getting most statistics the first days of April serves as observation epoch. The best detection efficiency is achieved when pointing the camera towards the zenith, because the light propagates through a thinner atmospheric layer [13].

Table 3: Proof simulation parameters

Parameter	Value
Observation date	2013.04.01 – 2013.04.10 2014.04.01 – 2014.04.10 2015.04.01 – 2015.04.10
Duration	11 h per day
Min. object size	0.1 m
Max. object size	100 m
Min. range	200 km
Max. range	4000 km
Geodetic latitude	48.78253 °
Geodetic longitude	9.19641 °
Geodetic altitude	355 m
Azimuth	0 °
Elevation	90 °

Diameter of Aperture	Lens dependent
FOV	System dependent
Number of pixels per row	Camera dependent
Pixel size	Camera dependent
Pixel FOV	System dependent
Exposure time	1 s
Gap time	Camera dependent
PSF	System dependent
Threshold parameter	2
Readout noise	Camera dependent
Dark noise	Camera dependent

3.1. Detection efficiency of different lenses

The most important quantity to determine besides the covered observation region is the size of the objects. A detection efficiency with respect of the object diameters can be generated from PROOF outputs. A big influence of the performance has the used camera lens. Best results are performed by camera lenses which are combining wide apertures and short focal lengths. The wider the aperture the more light reflected by a RSO is collected by the system. However, the focal length should be as short as possible. A longer focal length would increase the "speed" of an object on the camera sensor which causes shorter exposures of the RSO per pixel. However, short focal lengths would decrease the resolution.

Simulations are showing the detection efficiency for using different commercial available lenses equipped to the same camera (Andor Zyla) during an observation campaign from sunset until sunrise (Figure 3). For the used epoch the observation site is illuminated by the sun during the first and the last one and a half hours. This causes lower detection efficiencies for all object diameters and results in a detection efficiency below 50 %.
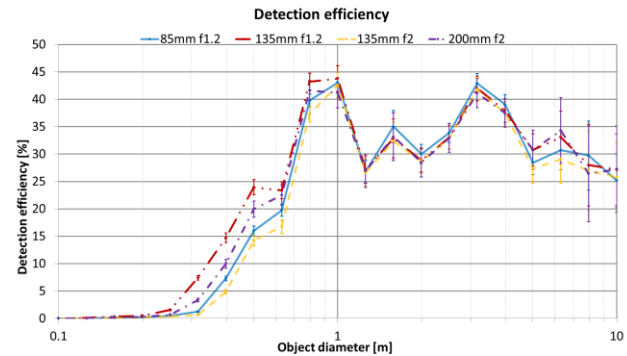

Figure 3: Detection efficiency for a system consisting of an Andor Zyla camera and different camera lenses simulated with PROOF (The data is the mean of 30 days observation in April with observation times from sunset to sunrise (11h).)

The simulated system efficiencies are roughly similar for RSOs larger 1 m in diameter. The maximum is about 45 % for 1 m objects. For smaller objects the efficiency drops quickly. At diameters below 1 m the lens parameters affects the performance most. While the 135 mm f/1.2 lens is able to detect RSO with diameters smaller 30 cm (5 % efficiency) the 135 mm f/2.0 lens reaches only 40 cm. The 85 mm f1.2 and 200 mm f/2.0 lenses are in between. In total the best performance of the simulated camera lenses is provided by the 135 mm f/1.2 lens due to the widest aperture (112.5 mm) and a short focal length.

3.2. Detection efficiency of different systems with the same FOV

For initial detection of RSOs the covered region of sky and therefore the FOV of the staring system must be as large as possible. The FOV depends on the chip size of the camera and the focal length of the used camera lens. Thus, the two system cameras have the same FOV with different lenses. A FOV of about 10 ° × 10 ° can be reached with the Andor Zyla camera equipped with the 85 mm f/1.2 lens, the FLI PL16803 with the 200 mm f/2.0 lens or a low cost CMOS-sensor which must be attached to the 50 mm f/1.2 lens due to its small size. In Figure 4, PROOF simulations are showing the slightly better performance of the Andor Zyla combination with respect to small object sizes. This is caused by the significantly smaller focal length, despite the 30 % smaller aperture diameter. The 50mm camera lens has a 60 % smaller aperture diameter than the 200 mm lens. This is why the low cost CMOS-sensor shows by far the worst results. For RSO sizes larger 1 m in diameter the detection efficiencies of all systems are similar.
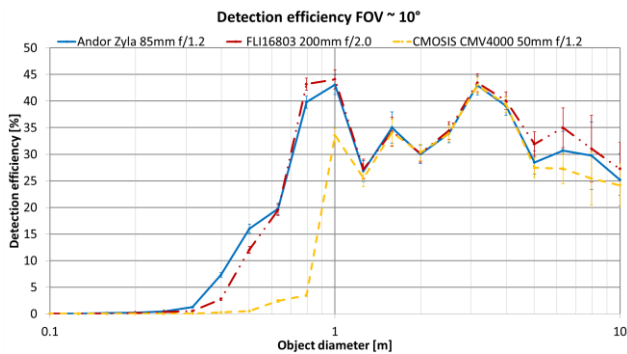
Figure 4: Detection efficiency for a staring system covering a FOV of about 10 ° × 10 ° simulated with PROOF. (The data is the mean of 30 days observation in April with observation times from sunset to sunrise (11h).)

It is possible to expand the covered region of sky with other combinations of lenses and cameras. But this extension is at the expense of detection efficiency. Figure 5 displays the results of systems with FOVs of about 15.5 ° × 15.5 °. Now, the Andor Zyla camera is equipped with the 50 mm f/1.2 lens and the FLI PL16803 with the 135 mm f/2.0 lens. To show the lost in detection efficiency the FLI PL16803 camera with the 200 mm lens from the simulations before is added as reference. The 50 mm f/1.2 camera lens shows the worst performance. Again a maximum efficiency of 45 % for 1m objects is still reached with the FLI camera and the probability for detecting a RSO with 0.5 m in diameter is 5 % for an observation from sunset to sunrise. Comparisons with the reference curve show the decreased detection efficiency, especially for small object sizes.
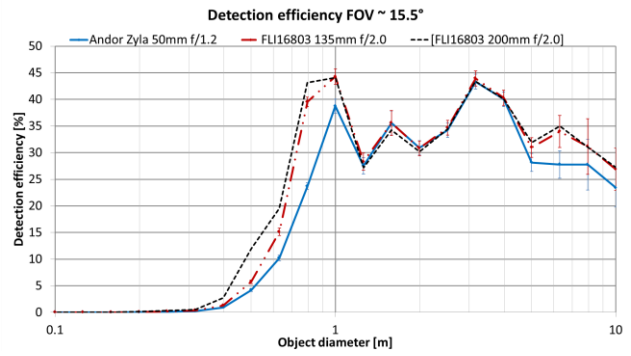
Figure 5: Detection efficiency for a staring system covering a FOV of about 15.5 ° × 15.5 ° simulated with PROOF. (The data is the mean of 30 days observation in April with observation times from sunset to sunrise (11h).)

4. MEASUREMENTS AND RESULTS

4.1. Staring performance

Performance analyzes were done for different staring system set-ups. Due to the lack of information about the geometric shape of an RSO the size information is based on the radar cross section (RCS), available for TLE-objects in the Satellite Catalog (SATCAT) [11]. A correlation to the optical size is given in [14].

Three observation campaigns with a total observation time of 11 h in July 2016 were conducted for a system set-up of the FLI PL16803 camera equipped with the 200 mm f/2.0 lens (FOV 10 ° × 10 °). The measurements are compared with TLE data for the same observation conditions and are shown in Figure 6. Furthermore, the calculated detection efficiency of these data is shown.
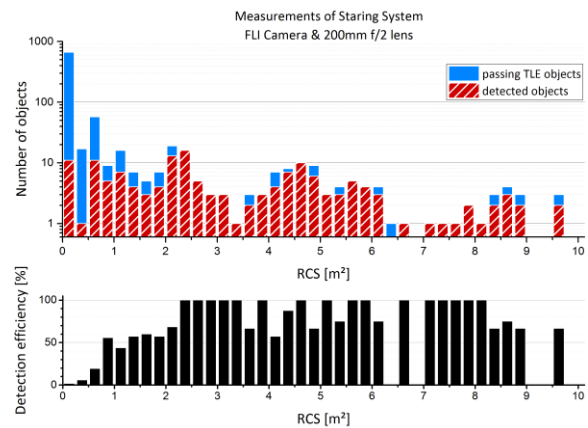
Figure 6: Detected objects of the staring system (FLI PL16803 camera & 200 mm f/2 lens) and theoretical FOV passes, based on TLE data as function of the radar cross section (Top). Detection efficiency of the measurements presented above (Bottom).

This system is able to detect RSOs in LEO with radar cross sections of all sizes despite the low detection efficiency for small objects. For radar cross sections above $0.5\,m^2$, the detection efficiency becomes greater than 50 %. In contrast to the simulations, real measurements show that the detection efficiency does not drop for RSOs larger than $2\,m^2$. The used gap time of 10 s between two images caused undetected crosses of

RSOs. Therefore drops in the detection efficiency occur in Figure 6.

During the observation, 199 objects crossed the FOV of the system at all. 157 RSOs are contained in the TLE database. Additional, 42 detected objects (21 %) have no corresponding entry and are not included in the analysis due to the missing information about the size. PROOF simulations are predicting 141 (±12) detections for the same parameters. With respect to the outdated space population model from 2009 used by PROOF and the increased number of RSOs (approx. 15 % since 2009), a similarity for the numbers of detections is recognizable. Previous measurements based on the FLI PL16803 camera equipped with the 135 mm f/2.0 lens are showing a similar agreement [15].

4.2. Recapturing of detected RSOs

A first successful series of recaptured RSOs took place in January 2016. The system was set up with the FLI PL16803 camera and the 135 mm f/2.0 lens. An exposure time for the streak detection was set to 1 s while a gap time between the images was 13 s due to the slow readout time of the camera. As staring camera direction a pointing at azimuth of 70° and an altitude of 50° were used. Figure 7 shows the detection of a track of a satellite in two subsequent images taken by the staring camera (left) and the "recaptured" object by the main telescope (right). The image processing algorithm was able to assign the detected track of the first image to the corresponding track in the second image and to extrapolate the trajectory for a short time prediction. Later analysis determined the object as GLOBALSTAR M003 (NORAD ID: 25165) at a range of 1922 km based on TLE information. In future, the high resolution image of the telescope can be used for more precise orbit determination. Space debris was detected with this Stare and Chase system as well, like the SL-16 R/B (NORAD ID: 23343) at a range of 759 km [13].
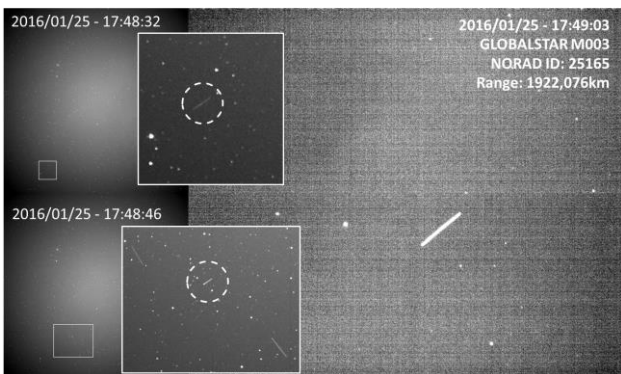

Figure 7: Successive images (exposure time 1 s) of the staring camera (FLI PL16803 camera & 135 mm f/2 lens) with tracks of the crossing RSO (left). Main telescope image (right) of the recaptured satellite GLOBALSTAR M0003 (NORAD ID: 25165) previously detected by the staring system.

Furthermore, successful recapture measurements were performed using the image processing algorithm which can handle short exposure times (<0.5 s). For this "recapture"-test the system was set up with the Andor Zyla camera and the 135 m f/2.0mm lens. Gap times between the image frames were set to 3 s and the exposure time was 0.1 s. A prediction headtime of 10 s and a line of sight

direction of 49° altitude and 333° azimuth were used. Figure 8 shows three images of the staring system (left) and the recaptured object through the telescope (right).
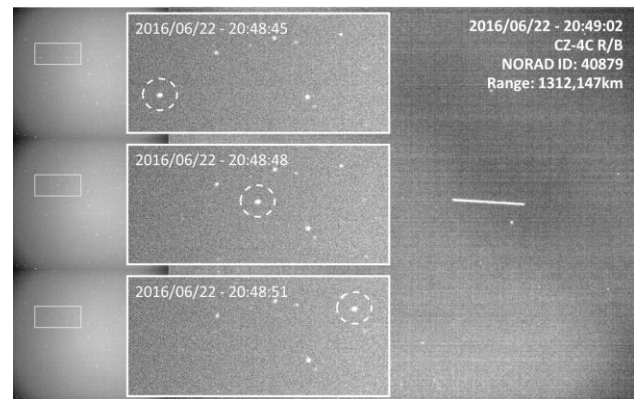

Figure 8: Successive images (exposure time 0.1 s) of the staring camera (Andor Zyla camera & 135 mm f/2 lens) with "dots" of the crossing RSO (left). Image of space debris CZ-4C R/B (NORAD ID: 40879) taken with the main telescope (right).

The captured RSO is space debris known as CZ-4C R/B (NORAD ID: 40879) at a range of about 1312 km from the DLR research observatory.

5. OUTLOOK

For the presented stare and chase system improvements of the location prediction algorithm are planned. Instead using an extrapolation based on a straight line fit a preliminary orbit can be determined. This orbit will also be valid just for a short time period due to the low resolution of the staring camera but a continuous tracking of the main telescope will be possible. This is necessary for laser ranging to new detected RSOs [10]. Further simulations will show the detection performance for different camera and lens combinations with the main goal of detecting smaller RSOs.

Furthermore, the staring system can be improved in respect to the covered observation area through upgrading it to a multi staring system with more than one camera. Such a Multi Staring System is presented in the following chapter.

5.1. Multi Staring System

The FOV of a staring system can easily be expanded by using multiple staring cameras. In order to avoid long telescope moving distances after a detection of a RSO and therefore long prediction headtimes a circular arrangement of the individual staring FOVs is supposed with an initially telescope direction to the center point. The alignments of the cameras cause due to the rectangular or square shaped FOVs a polygonal shaped observation region. An example for a multi staring system with five cameras is given in Figure 9.
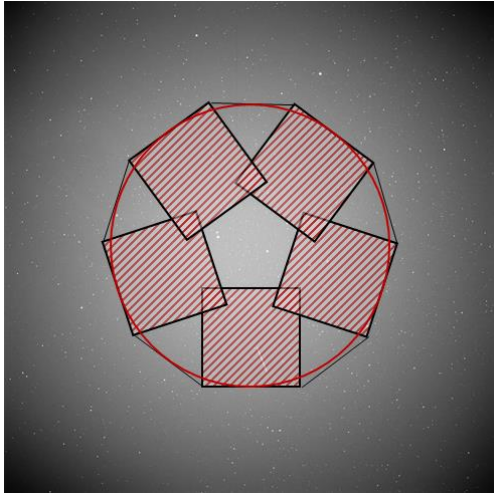
Figure 9: Suggested camera alignment for a multi staring system of five cameras with overlapping FOVs (hatched areas).

For a multi staring system the surveillance area depends on the number of used cameras and their FOVs. FOVs of about 10°×10° (Andor Zyla & 85 mm lens or FLI PL16803 & 200 mm lens) and 15.5°×15.5° (Andor Zyla 50 mm lens or FLI PL16803 & 135 mm lens) are possible with the available hardware. In contrast to a single camera with FOV of 10°×10°, a 5 camera system increases the covered region from 5.64° to 14.59° in diameter (approximated to a circle). For a camera FOV of 15.5°×15.5° the region is expanded from 8.75° to 22.61°.

Performances regarding the detectable object size remain unchanged to a single camera system but the larger observation area in sky allows detecting more RSOs. Table 4 shows the theoretical number of various, FOV-crossing TLE objects per day and in one year based on the TLE-catalog (about 15500 entries in 2016) for different staring systems. Compared are systems set-ups with single cameras to multi staring systems containing 5 cameras. The systems are pointing to zenith and the effective FOVs are approximated by circles.

Table 4: Number of crossing TLE objects per day and per year for different staring systems with a total number of about 15500 RSOs in the TLE catalog (as of 2016).

No. of cameras	FOV = 10° × 10°		FOV = 15.5° × 15.5°	
	1 day	1 year	1 day	1 year
1	2233	13248	3422	13334
5	5480	13390	7977	13465

Per day, the number of crossing objects is more than doubled if 5 cameras are used instead of one. In one year the numbers are similar but a multi staring system would be able to detect each object more often.

6. CONCLUSION

The presented system is able to find unknown orbiting objects and generate sufficiently precise predictions of the objects trajectory for further measurements with a high resolution telescope. Already existing observation sites can easily be upgraded with a staring camera. Low costs and flexibility in adjusting the system to different requirements are reached with easily exchangeable off-the-shelf components.

Based on the simulations, it can be assumed that the combination of the FLI PL16803 and the 135 mm f/2.0 lens is a good system for LEO surveillance. Its large FOV compensates the weakness for detecting small objects. Is the focus on detecting small objects the Andor Zyla camera should be equipped with the 135 mm f/1.2 lens (see Figure 3)

This Stare and Chase-system in combination with satellite laser ranging can be an alternative optical system for initial LEO surveillance. Its independence of prior information about RSO orbits and the wide FOV allows this system to support a buildup or maintenance of a space object catalog.

7. REFERENCES

[1] J.-C. Liou, editor, "Update on Three Major Debris Clouds", Orbital Debris Quarterly News, 14(2), April 2010, www.orbitaldebris.jsc.nasa.gov.

[2] J.-C. Liou, editor, "Increase in ISS Debris Avoidance Maneuvers", Orbital Debris Quarterly News, 16(2), April 2012, www.orbitaldebris.jsc.nasa.gov.

[3] P. Anz-Meador, editor, "Top Ten Satellite Breakups Reevaluated", Orbital Debris Quarterly News, 20(1&2), January/April 2016, www.orbitaldebris.jsc.nasa.gov.

[4] Handbook for Limiting Orbital Debris, NASA Handbook 8719.14, approved 2008-07-30

[5] J.R. Shell, "Optimizing orbital debris monitoring with optical telescopes", in 2010 AMOS Conference, 2010

[6] M. Laas-Bourez, et al., „A new algorithm for optical observation of space debris with the TAROT telescopes", Advances in Space Research, Volume 44, 2009

[7] Wang Jian-li, et al., "Large FOV Mobile E-O Telescope for Searching and Tracking Low-orbit Micro-satellites and Space Debris", CNKI Journal, Chinese Journal of Optics, 02/2011

[8] L. Cibin, et al., "Wide Eye Debris telescope allows to cataloque objects in any orbital zone", Mem. Soc. Astron. It. Suppl., vol. 20, p. 50, 2012

[9] M. Boër, "The MetaTelescope: a System for the Detection of Objects in Low and Higher Earth Orbits", in 2015 AMOS Conference, 2015

[10] D. Hampf, et al., „First successful satellite laser ranging with a fibre-based transmitter", Advances in Space Research, Volume 58, 2016

[11] https://celestrak.com/, provided by the Center for Space Standarts & Innovation (CSSI)

[12] Sven Flegel, "Maintenance of the ESA MASTER Model" Institute of Aerospace Systems, TU Braunschweig, Final Report, 21705/08/D/HK, 2011

[13] Thomas Hasenohr, "Initial Detection and Tracking of Objects in Low Earth Orbit", Masterthesis, in preparation 2016

[14] G. D. Badhwar, P. D. Anz-Meador, "Relationship of Radar Cross Section to the Geometric Size of Orbital Debris", in AIAA/NASA/DOD Orbital Debris Conference, 1990

[15] Paul Wagner, Daniel Hampf, Wolfgang Riede, "Passive optical space surveillance system for initial LEO object detection", in 66th International Astronomical Conference, 2015